EGTRIB Journal
JOURNAL OF
THE EGYPTIAN SOCIETY OF TRIBOLOGY
VOLUME 19, No. 3, July 2022, pp. 1 - 9 **ISSN 2090 - 5882**
(Received April 19. 2022, Accepted in final form June 07. 2022) **www.egtribjournal.com**

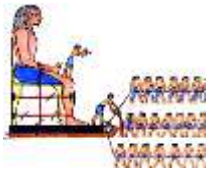

EFFECT OF THE CONTACT FORCE ON VOLTAGE OUTPUT OF A TRIBOELECTRIC NANOGENERATOR

Al-Kabbany A. M. and Ali W. Y.

Department of Production Engineering and Mechanical Design, Faculty of Engineering, Minia University.

ABSTRACT
Triboelectric generators (TENG) are seen as a great way to make green energy harvesters and self-powered sensors. With the rapid development of TENG, a theoretical model that accounts for the contact force in a contact and separation of TENG is needed. This study aims at establishing a theoretical model that can be applied to one specific TENG and predict the value of the output open-circuit voltage after being activated by a specific contact force.

A model that links the output open-circuit voltage of a TENG and the contact force was established, then experiments were performed to test the model. It was found that the presented model correctly predicts the type of trend that links the open-circuit voltage and the force and also the value of the open-circuit voltage of a specific TENG under a specific contact force.

KEYWORDS
Triboelectric nanogenerator, contact force, voltage.

INTRODUCTION
When 2 dielectric materials come into contact with one another, charges are transferred from one material to the other creating a net positive charge on one dielectric, and a net negative charge on the other dielectric. That effect is known as triboelectrification, [1 - 4], where the intensity and sign of the charges accumulating on each of the dielectrics are determined by their position in the triboelectric series, [5 - 7], that rank materials by their likelihood to gain a positive or negative charge. That effect can be used to produce energy using a device known as triboelectric nanogenerators (TENG), [8]. They are made by adding electrodes to one of the surfaces of each one of the dielectrics.

TENG have two main uses, as self-powered sensors, [9 - 12], and as generators, [13 - 16]. Even though the phenomenon of triboelectrification itself is poorly understood, this has not stopped many theoretical models from being made that try to predict many output characteristics of TENG, [17 - 18]. The theoretical models used Maxwell's equations to come up with a theoretical understanding of TENGs. It was identified that the V-Q-x equation, links the open-circuit voltage produced by a TENG (V_{oc}), the charge generated on each

dielectric (*Q*), and the separation distance between the two dielectric surfaces after contact (*x(t)*), [19].

Those models did not take into consideration the effect of the contact force (*F*) on the output voltage. Two subsequent models took the contact force into account, [20 - 21], where those models showed good results, but could not provide a full accounting of the experimental results and were too general in their scope. The present study aims at introducing a theoretical model that depends on results of the experiments done on specimens of the two dielectrics of a specific contact and separation TENG. The results of the experiments can then be used to fill in an equation, that can be used to predict the V_{oc} of the TENG at any force.

Equation derivation:
It can be assumed that the amount of generated charge, and thus the charge density (σ), on any of the dielectrics of the TENG correlates linearly with the actual contact surface area (*A*), [22]. This can be expressed in equation (1).

$$\sigma \propto A \qquad (1)$$

Also, *A* was found to increase almost linearly and rapidly with small values of *F*, until the increase in *A* with a constant increase in *F* starts to plateau, [20, 23]. This can be interpreted as a correlation between *A* and *F* expressed in equation (2), where β is a system-specific exponent that is always less than 1. This is a fair assumption considering any graph following the general formula of $y = Ax^B$ seems to give the best explanation for the results in the previous work, [23]. Because the first part of the graph is always very close to a linear relationship, an equation following the form of $y = A\ ln(x) + b$ would also give a similar result. However, it would also result in a zero value of *A* at a non-zero value of *F* and is thus deemed to be an unworthy candidate for explaining the relationship between *F* and *A*.

$$A \propto F^{\beta} \qquad (2)$$

The deformation of asperities under loading can bring the 2 materials closer by a few microns, therefore, once the load is removed, and the TENG returns to its original position, the separation distance will be slightly higher, this will slightly increase the voltage generated, however, this mechanism is expected to increase the voltage by a negligible amount.

From equations (1) and (2), we can get equation (3), and from equation (3), we can get equation (4), where the specific charge density σ_s is the amount of charge per unit area generated on any of the dielectrics of a specific TENG while being applied on by a unit force, note that *F* in equation (4) is assumed to be multiplied by a constant equal to $1N^{-1}$, in order to balance the dimensions of the equation.

$$\sigma \propto F^{\beta} \qquad (3)$$

$$\sigma = \sigma_s F^{\beta} \qquad (4)$$

The induced open-circuit voltage is described by the equation $V_{oc} = \frac{\sigma x(t)}{\varepsilon_o}$, where ε_o is the permittivity of vacuum, [19]. Using equation (4), we can conclude equation (5) that describes the relationship between the V_{oc} of a TENG and F.

$$V_{oc} = \frac{\sigma_s x(t)}{\varepsilon_o} F^{\beta} \qquad (5)$$

Experimental Verification

Five 60 mm by 60 mm specimens were prepared. The first was made of PMMA with a surface roughness R_a of 1.134 µm, the second was made of Kapton with a surface roughness R_a of 1.354 µm, while the third was made of PTFE with a surface roughness R_a of 1.351 µm. Those three specimens had aluminum foil covering one side to harvest the generated charge. The two other specimens were made, each of of these two had three layers, a Kapton layer, followed by an aluminum foil layer, then a sandpaper layer. The first of those two specimens had a sandpaper with a grit of 180, the other had sandpaper of a 320 grit. the PMMA specimen was attached to a load cell to measure the force acting on it, while the each of the four specimens was attached one at a time to a sponge, which was attached to a wooden plate that could move up and down. Each of the specimens was then pressed on the PMMA specimen, then they were separated by a distance of 60 mm, noting that the equation deduced above may not work at this separation distance. However, it is assumed that it does. This was repeated 56 times, where the force applied on the PMMA specimen was measured using a load cell connected to an HX711 ADC chip connected to an Arduino Uno. The voltage at separation generated between the two specimens was measured using the Arduino Uno, the forces applied were often smaller that 1N, because the higher the value of the force, the more linear the hypothesized relationship becomes and the harder it is to clearly distinguish it from an actual linear relationship. This can be seen clearly in a graph that plots the relationship as $y = \frac{d}{dx}(Ax^B)$.

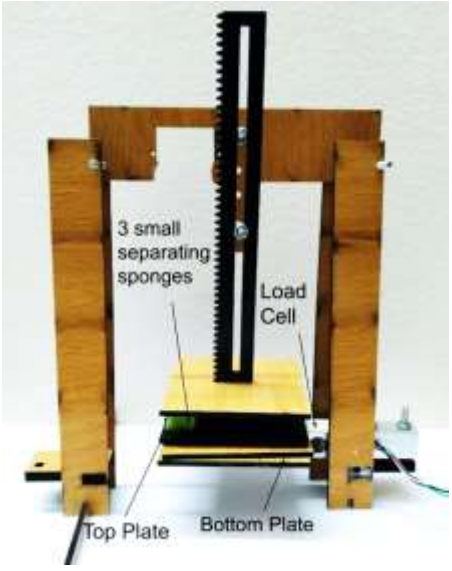

Fig. 1 The test rig used in the experiment.

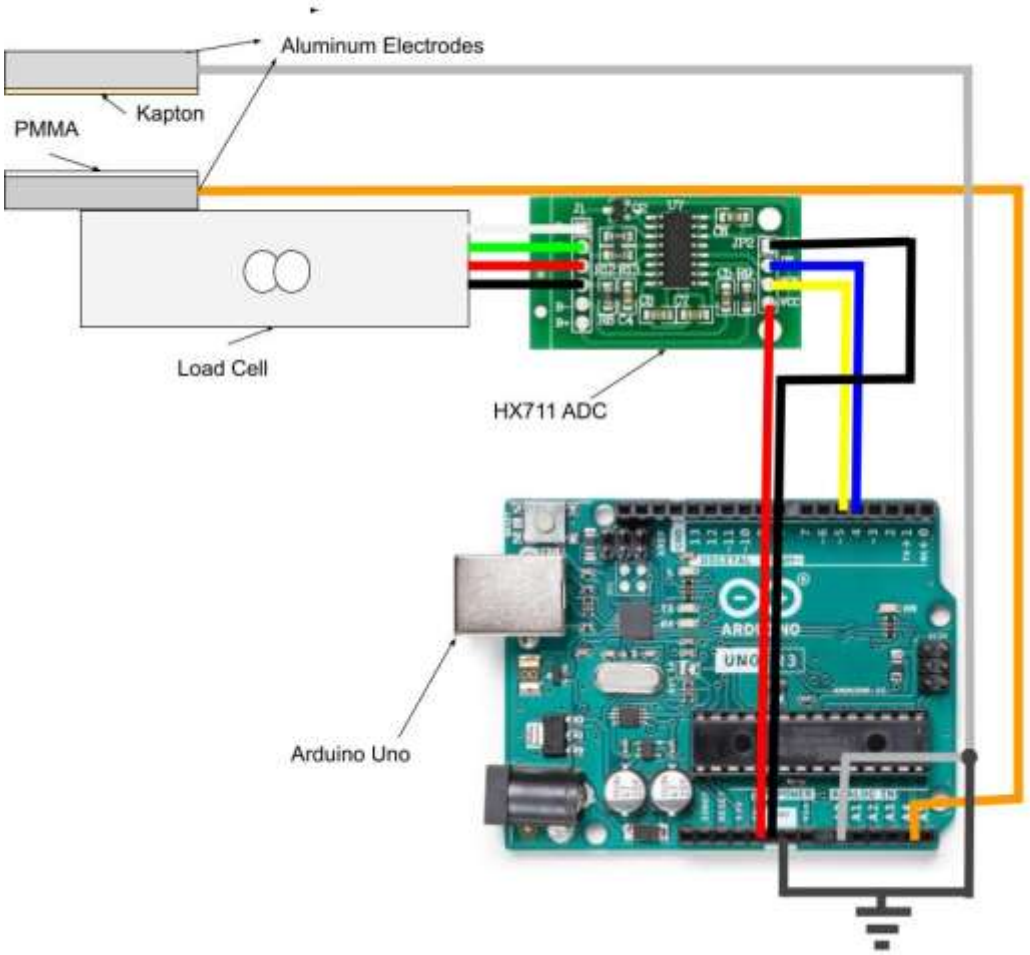

Fig. 2 Schematic of the circuit used to measure the contact force and open-circuit voltage generated by the TENG.

RESULTS AND DISCUSSION

The 56 points of force versus voltage for each specimen were arranged in ascending order according to the contact force, and the average force and voltage of each eight consecutive points were calculated. The contact force was plotted on the x-axis while the open-circuit voltage was plotted on the y-axis, with a power trendline following the general formula $y=Ax^b$, the results are shown in Fig. 3 to Fig. 7.

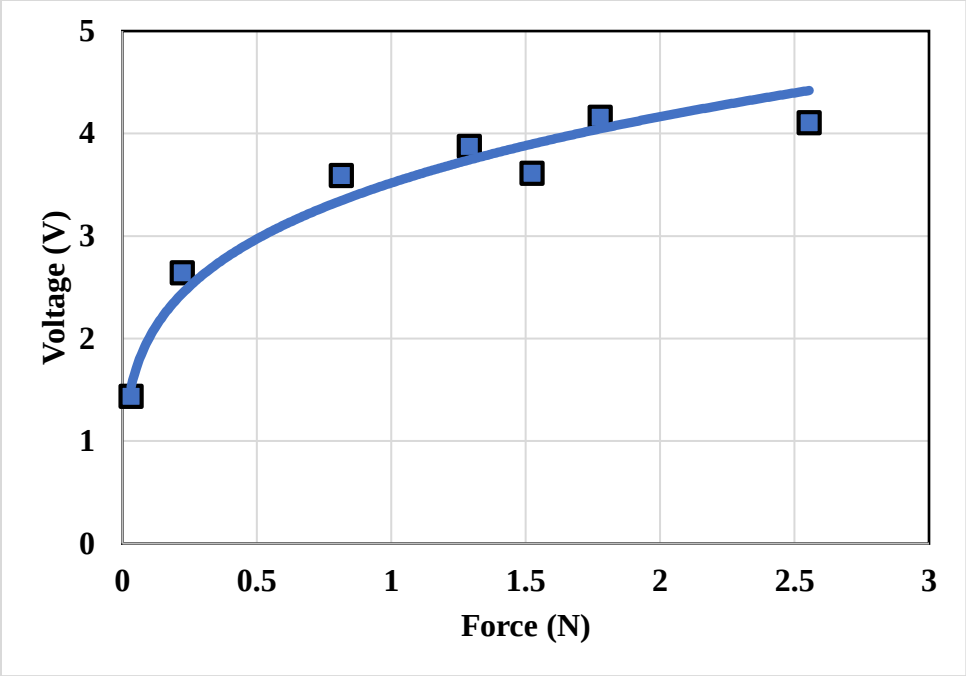

Fig. 3 Voltage vs Force graph for Kapton specimen with no sandpaper in contact with PMMA.

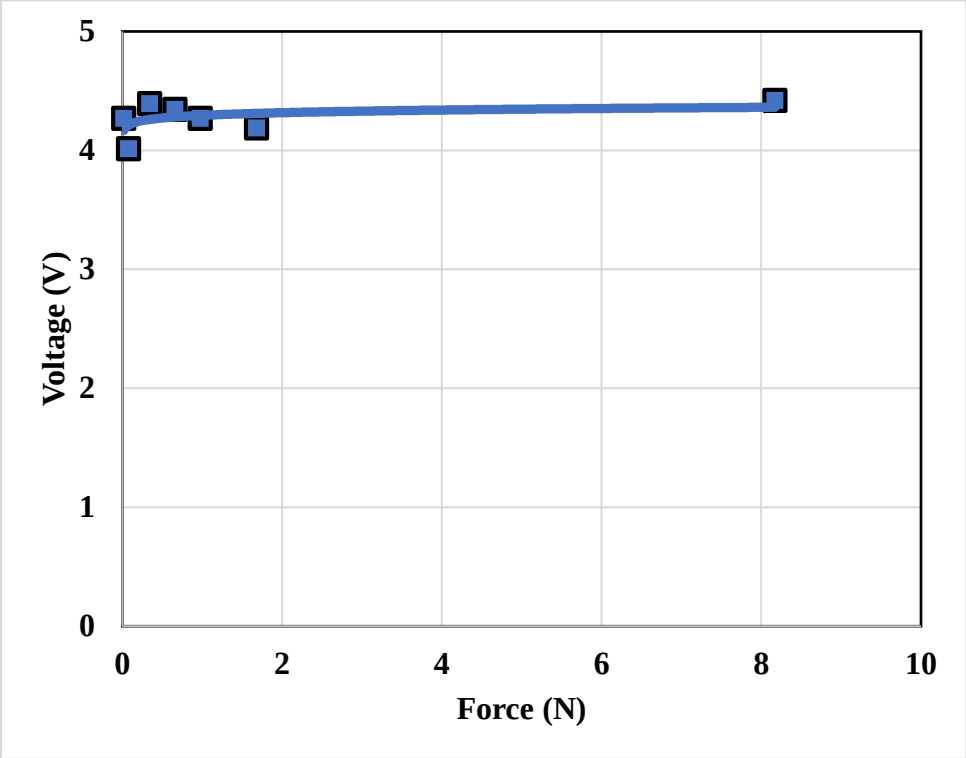

Fig. 4 Voltage vs Force graph for PTFE specimen with no sandpaper in contact with PMMA.

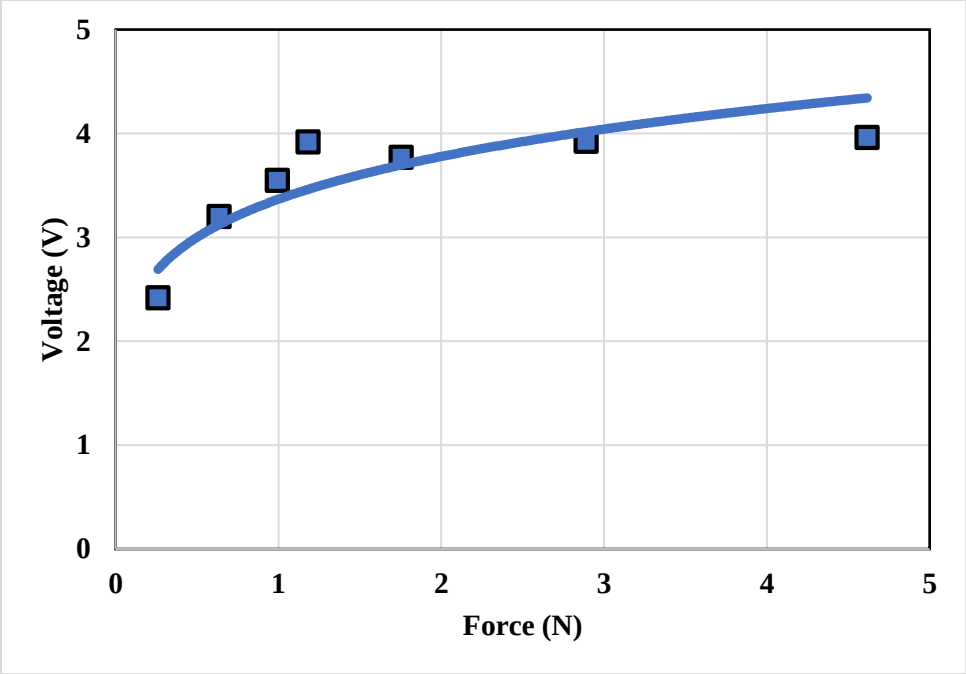

Fig. 5 Voltage vs Force graph for Kapton specimen with 180-grit sandpaper in contact with PMMA.

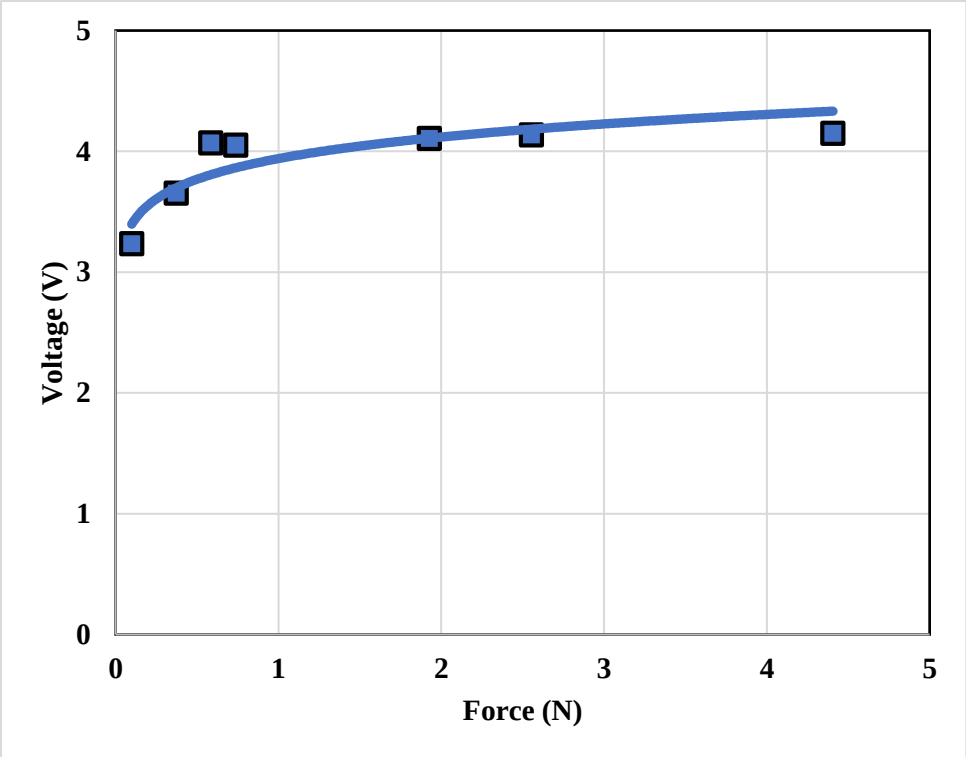

Fig. 6 Voltage versus Force graph for Kapton specimen with 320-grit sandpaper in contact with PMMA.

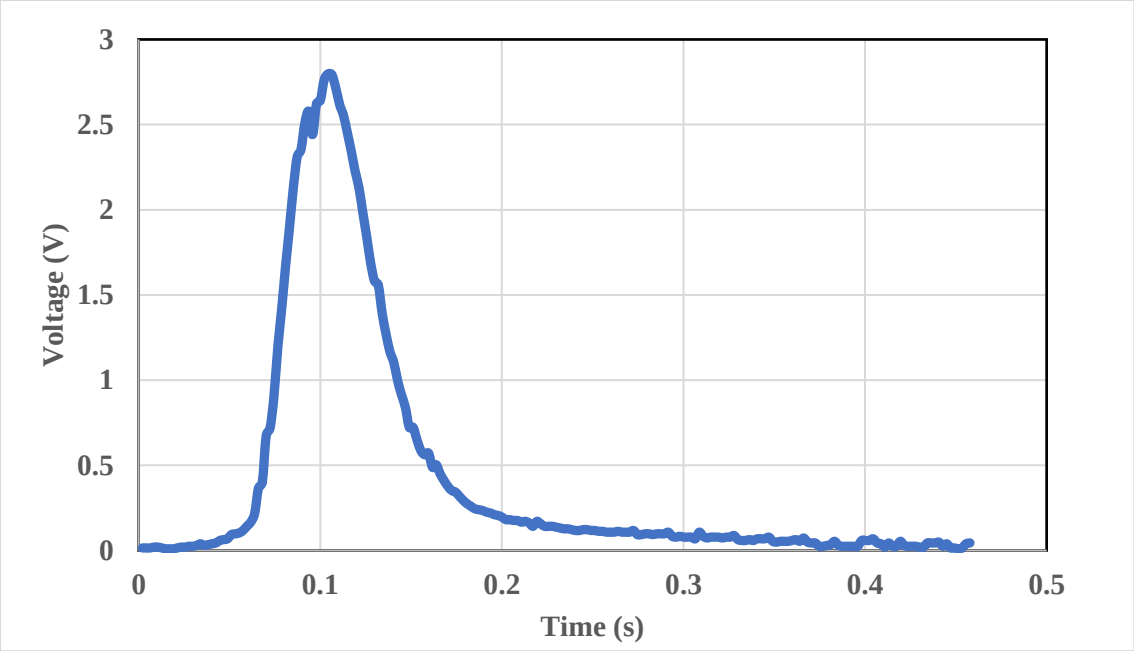

Fig.7, Example of a voltage pulse at separation.

To find an appropriate trendline to add to the graph, the R-Squared value of every possible trendline was examined, and it was found that a logarithmic or a power trendline were the best fitting trendlines for each of the above graphs except for the one with the PTFE specimen (which will be discussed later), however, a power trendline was seen as a better choice for the reason mentioned above, this also shows that a linear relationship between open-circuit voltage and contact force is unlikely to be true, the equation for each power and linear trendline was also obtained, and the values of σ_s and β were calculated for each graph, this is shown in table 1.

Table 1, Analysis of the 4 graphs.

Material used with PMMA	R^2 value for a power trendline	R^2 value for a linear trendline	Equation of the power trenline	σ_s (C/m^2)	β
Kapton (no sandpaper)	$R^2 = 0.9496$	$R^2 = 0.7241$	$y = 3.5175x^{0.2435}$	5.1883125×10^{-10}	0.2435
PTFE	$R^2 = 0.2137$	$R^2 = 0.225$	$y = 4.2944x^{0.0075}$	6.33424×10^{-10}	0.0075
Kapton (180-grit sandpaper)	$R^2 = 0.7586$	$R^2 = 0.4602$	$y = 3.3672x^{0.1662}$	4.96662×10^{-10}	0.1662
Kapton (320-grit sandpaper)	$R^2 = 0.768$	$R^2 = 0.3897$	$y = 3.9397x^{0.064}$	5.8110575×10^{-10}	0.064

Two distinct observations can be made from the above table. The first is that the value of the constant β was with the specimen made of PTFE, as the PTFE used was much softer than the Kapton, and thus had a lower modulus of elasticity which allowed its asperities to deform easily upon contact. Increasing the value of the actual contact surface area, which in turn caused the value of the open-circuit voltage to be high even at low forces, decreased the value of β. This shows evidence that there is a direct relationship between β and the moduli of elasticity of the materials used in the TENG, the low value of β is the reason why a linear

relationship had a high R^2 value in this experiment, but it is thought that if those experiments were done at an even lower load, the power relationship would be more apparent. The beginning of this decline in the open-circuit voltage can also be seen at the left-hand side of Fig. 4, where the open-circuit voltage is thought to start decreasing rapidly at lower loads than the ones tested.

The second observation is that the value of σ_s was lower in the case of the Kapton specimen with the 180-grit sandpaper than the Kapton specimen with the 320-grit sandpaper, since the 180-grit sandpaper has fewer asperities than the 320-grit sandpaper, this can be seen as evidence that the number of asperities on a surface causes an increase in σ_s.

CONCLUSIONS

This study presents a theoretical model that can be applied to a specific system to predict the open-circuit voltage of a TENG that accounts for the contact force. This was not the first model to not predict the shape of the curve, but it offered a way to predict the open-circuit voltage of a specific TENG based on two constants, where the output of the TENG depends on its constants σ_s and β. The constant σ_s is thought to depend on the position of the materials chosen in the triboelectric series and on the number of asperities on each surface, while the exponent β is thought to depend on the elastic moduli of the chosen materials, where more studies are needed to confirm the usability of this model, and test the variables that could influence the constant σ_s and the exponent β.

REFERENCES

1. Al-Qaham, Y., Mohamed M. K., and Ali. W. Y., "Electric Static Charge Generated From the Friction of Textiles", Journal of the Egyptian Society of Tribology, EGTRIB, Vol. 10, No. 2, pp. 45 - 56, (2013).

2. Shivangi N., Mukherjee R., and Chaudhuri B., "Triboelectrification: A review of experimental and mechanistic modeling approaches with a special focus on pharmaceutical powders", International journal of pharmaceutics Vol. 510, No. 1, pp. 375-385, (2016).

3. Ali A.S., "Triboelectrification of Synthetic Strings", Journal of the Egyptian Society of Tribology, EGTRIB, Vol. 16, No. 2, pp. 26-36, (2019). 4. Zou, Haiyang, et al., "Quantifying the triboelectric series", Nature communications, Vol. 10, No. 1, pp. 1427, (2019).

4. Pan S. and Zhang Z., "Fundamental theories and basic principles of triboelectric effect: a review." Friction, Vol. 7, No. 1, pp. 2-17, (2019)

5. Zou H., Zhang Y., Guo L., Wang P., He X., Dai G., Zheng H., Chen C., Wang A. C., Xu C. and Wang Z. L., "Quantifying the triboelectric series", Nature communications, Vol. 10, No. 1, pp. 1427, (2019).

6. Diaz A. F., and Felix-Navarro R. M., "A semi-quantitative tribo-electric series for polymeric materials: the influence of chemical structure and properties", Journal of Electrostatics, Vol. 62, No. 4, pp. 277-290, (2004).

7. Burgo, Thiago AL, Galembeck F., and Pollack G. H., "Where is water in the triboelectric series?", Journal of Electrostatics Vol. 80, pp. 30 - 33, (2016).

8. Wu C., Wang A. C., Ding W., Guo H. and Wang Z. L., "Triboelectric nanogenerator: a foundation of the energy for the new era.", Advanced Energy Materials, Vol. 9, No .1, 1802906, (2019).

9. Jin T., Sun Z., Li L., Zhang Q., Zhu M., Zhang Z., Yuan G., Chen T., Tian Y., Hou X. and Lee C., "Triboelectric nanogenerator sensors for soft robotics aiming at digital twin applications.", Nature communications, Vol. 11, No .1, pp, 1-12, (2020).
10. Qin K., Chen C., Pu X., Tang Q., He W., Liu Y., Zeng Q., Liu G., Guo H. and Hu C., "Magnetic array assisted triboelectric nanogenerator sensor for real-time gesture interaction.", Nano-micro letters, Vol. 13, No. 1, .pp. 1-9, (2021).
11. Zhou Q., Pan J., Deng S., Xia F. and Kim T., "Triboelectric Nanogenerator-Based Sensor Systems for Chemical or Biological Detection.", Advanced Materials, Vol. 33, No. 35, 2008276, (2021).
12. Dhakar L., Pitchappa P., Tay F. E. H. and Lee C., "An intelligent skin based self-powered finger motion sensor integrated with triboelectric nanogenerator.", Nano Energy, Vol. 19, pp, 532-540, (2016).
13. Yang Y., Zhu G., Zhang H., Chen J., Zhong X., Lin Z. H., Su Y., Bai P., Wen X. and Wang Z. L., "Triboelectric nanogenerator for harvesting wind energy and as self-powered wind vector sensor system.", ACS nano, Vol. 7, No. 10, pp. 9461-9468, (2013).
14. Zhang H., Yang Y., Su Y., Chen J., Adams K., Lee S., Hu C. and Wang, Z. L., "Triboelectric nanogenerator for harvesting vibration energy in full space and as self-powered acceleration sensor.", Advanced Functional Materials, Vol. 24, No. 10, pp. 1401-1407, (2014) .
15. Cheng P., Guo H., Wen Z., Zhang C., Yin X., Li X., Liu D., Song W., Sun X., Wang J. and Wang Z. L., "Largely enhanced triboelectric nanogenerator for efficient harvesting of water wave energy by soft contacted structure.", Nano Energy, Vol. 57, pp. 432-439, (2019).
16. Wang X., Niu S., Yin Y., Yi F., You Z. and Wang Z. L., "Triboelectric nanogenerator based on fully enclosed rolling spherical structure for harvesting low-frequency water wave energy.", Advanced Energy Materials, Vol. 5, No. 24, 1501467, (2015).
17. Wang Z. L., Jiang T. and Xu L., "Toward the blue energy dream by triboelectric nanogenerator networks.", Nano Energy, Vol. 39, pp. 9-23, (2017).
18. Dharmasena R. D. I. G., Jayawardena K. D. G. I., Mills C.A., Dorey R. A. and Silva S. R. P., "A unified theoretical model for Triboelectric Nanogenerators.", Nano Energy, Vol. 48, pp. 391-400, (2018).
19. Niu S., Wang S., Lin L., Liu Y., Zhou Y. S., Hu Y. and Wang Z. L., "Theoretical study of contact-mode triboelectric nanogenerators as an effective power source.", Energy & Environmental Science, Vol. 6, No. 12, pp. 3576-3583, (2013).
20. Xu Y., Min G., Gadegaard N., Dahiya R. and Mulvihill D. M., "A unified contact force-dependent model for triboelectric nanogenerators accounting for surface roughness.", Nano Energy, Vol. 76, 105067, (2020).
21. Vasandani P., Mao Z. H., Jia W. and Sun M., "Relationship between triboelectric charge and contact force for two triboelectric layers.", Journal of Electrostatics, Vol. 90, pp. 147-152, (2017).
22. Min G., Xu Y., Cochran P., Gadegaard N., Mulvihill D. M. and Dahiya R., "Origin of the contact force-dependent response of triboelectric nanogenerators.", Nano Energy, Vol. 83, 105829, (2021).
23. Helseth, L. E., "Optical force sensing principle based on transparent elastomer with a rough surface.", Sensors and Actuators A: Physical, Vol. 263, pp. 667-676, (2017).